

Graphite Intercalation Compound Associated with Liquid Na-K Towards Ultra-Stable and High-Capacity Alkali Metal Anodes

Leyuan Zhang¹, Sangshan Peng¹, Yu Ding¹, Xuelin Guo¹, Yumin Qian¹, Hugo Celio¹, Gaohong He², and Guihua Yu^{1*}.

¹Materials Science and Engineering Program and Department of Mechanical Engineering, The University of Texas at Austin, Austin, TX 78712, USA

²State Key Laboratory of Fine Chemicals, R&D Center of Membrane Science and Technology, School of Chemical Engineering, Dalian University of Technology, Dalian, 116023 China

* Correspondence to: ghyu@austin.utexas.edu.

Experimental

NaK-G-C and MK-G-C electrodes synthesis

The Na-K liquid was prepared by mixing 33 wt% Na and 67 wt% K in a vial at room temperature. After several minutes, sodium and potassium solids were melted to be a uniform liquid with silver-shiny color. However, due to the trace of oxygen existed in the glovebox, an ash black layer was covered on the surface. The NaK-G-C electrode was synthesized by mixing disks of carbon paper (diameter: ~11 mm) and liquid drop of Na-K in a vial at room temperature. Ascribing to the capillary effect, good wetting behavior and high surface tension of liquid Na-K, the fast penetration of liquid into the carbon matrix was observed. After several minutes, the color of carbon paper was turned to be gold. Finally, plenty of shiny electrodes covered by the liquid alloy on the surface could be easily made within ~10 minutes. The MK-G-C electrode was also prepared by immersing disks of carbon paper into molten K at 100-150 °C. The penetration of K through the whole matrix was completed within seconds. Similarly, the diffusion of molten Li into carbon papers was found at 250-300 °C. However, sodium was not able to diffuse into the carbon matrix.

Cathode materials synthesis

The synthesis of VOPO₄ nanosheets was the same as reported in our previous work¹. The bulk VOPO₄·2H₂O chunks were first dispersed in 2-propanol with a certain concentration and then ultrasonicated in water for 30 mins. The yellow color of original dispersion faded during the ultrasonication, indicating the exfoliation of VOPO₄. The A₂MnFe(CN)₆ (A: Na or K) was synthesized by a precipitation method, which was previously reported by Goodenough and coworkers^{2, 3}. For the activated carbon powder, it was purchased from MTI (TF-B520) and directly used without any treatment. The polysulfide (Li₂S₈) solution was obtained by mixing Li₂S and S in 1:1 DOL/DME solvent together with 1M potassium bis(trifluoromethanesulfonyl)imide (KTFSI) and 0.1M KNO₃. The T-Nb₂O₅/rGO material was prepared by the solvothermal process and annealing treatment, as reported in the previous work. The homogeneous mixture of GO powder and NbCl₅ in ethylene glycol (EG) was heated at 180°C for 24 h to obtain the Nb₂O₅/rGO colloidal suspension. Then, after an annealing treatment for 3 h in Ar flow, the final product was highly crystalline T-Nb₂O₅ with reduced GO, named T-Nb₂O₅/rGO.

Electrochemical measurement

The NaK-G-C, MK-G-C, K-metal and Na-metal electrodes were each assembled into symmetric cells with Celgard separators for the cycling test of alkali metal stripping/deposition. The used K-ion electrolyte was 1 or 2 M KFSI in 1:1 EC/DEC. The Na-ion electrolyte was 1 M NaClO₄ in 1:1 EC/DEC. To evaluate the full battery performance, the CR2032 coin cells were assembled with NaK-G-C anode, glass-fiber separator and as-prepared cathode. For the preparation of VOPO₄ electrode, carbon black and sodium carboxymethyl cellulose (CMC) were directly added into aforementioned 2-propanol solution after ultrasonication (VOPO₄: Super P: CMC = 80: 15: 5 wt%). The typical loading of VOPO₄ on the Al foil is 0.5~1 mg cm⁻². The uniform slurry of 80 wt% AC, 10 wt% carbon black and 10 wt% polyvinylidene fluoride (PVDF) was prepared by adding N-methyl-2-pyrrolidinone (NMP) solvent and thoroughly mixing in a Thinky Mixer AR-100. After coating onto the Al foil, it was dried in vacuum at 95 °C overnight. The typical AC loading was about 3 mg cm⁻² for electrochemical tests. The preparation of T-Nb₂O₅/rGO electrodes was similar to the AC electrode. 80 wt% T-Nb₂O₅/rGO, 10 wt% carbon black and 10 wt% PVDF were uniformly mixed in the NMP solvent and coated onto the Cu foil or carbon paper disks. The typical loading of active materials is around 1 mg cm⁻². The K₂MnFe(CN)₆ or Na₂MnFe(CN)₆ cathode electrodes were consisted of 60 wt% cathode materials, 30 wt% carbon black and 10 wt% CMC binder. After adding a certain amount of water as the solvent, the resultant slurry was uniformly mixed and coated onto carbon-coated Al foil. Then the

electrodes were dried in vacuum overnight. The typical loading of active materials was 0.5~1 mg cm⁻². The polysulfide electrode was prepared by dipping the solution into carbon paper discs. The area of each cathode electrode was around 1 cm². The electrolytes employed in full battery were 2 M KFSI in 1:1 EC/DEC, saturated KClO₄ in PC with 2 wt% FEC or 1M NaClO₄ in PC with 2 wt% FEC. Additionally, the electrolyte for the polysulfide cathode was 1M KTFSI in 1:1 DOL/DME. All coin cells were assembled in the glovebox and tested at room temperature with LAND, Arbin battery test systems or BioLogic VMP3 potentiostat. The C rates are defined as follows: VOPO₄ (1C: 160 mA g⁻¹), K₂MnFe(CN)₆ (1C: 160 mA g⁻¹), and Na₂MnFe(CN)₆ (1C: 120 mA g⁻¹). The transparent cell was probed using a Nikon Epiphot 200 microscope. For constructing the pouch format battery, one 4 cm × 4 cm- or 4 cm × 5 cm-sized NaK-G-C anode and one 4cm×4cm-sized K₂MnFe(CN)₆ cathode were used as electrodes with one 5.5~6 cm × 7 cm glass-fiber separator and 600 μl of saturated KClO₄ in PC with 2% FEC as the electrolyte.

Materials characterizations

X-ray powder diffraction (XRD) patterns were performed on a Rigaku MiniFlex 600 equipped with Cu K α radiation ($\lambda = 1.5406 \text{ \AA}$). For the air-sensitive samples, they were sealed by the X-ray transparent film (Kapton or Mylar) in the Ar-filled glovebox before the measurement. The morphology observations of carbon paper were carried out on a Hitachi scanning electron microscope (SEM, S-5500) and the morphologies and energy-dispersive spectroscopy (EDS) analysis of NaK-G-C electrodes were observed by FEI Quanta 650 ESEM equipped with Oxford EDS system. To analyze the chemical composition of NaK-G-C during the preparation and characterize the interface components of NaK-G-C electrodes after cycling, the XPS spectra were collected on a Kratos AXIS Ultra XPS spectrometer. All binding energies were referenced to the C1s peak of 284.8 eV. The air-tight container filled with Ar gas was used for the transfer of air-sensitive samples from the glovebox. For electrodes after cycling in the symmetric cell, they were rinsed thoroughly in EC/DEC before the measurement.

DFT simulations

Electron configurations of all the molecules were calculated by DFT method within the framework of the Gaussian 09 package. The standard Pople basis set, 6-31G++(d,p), combined with the Lee-Yang-Parr exchange correlation functional (B3LYP) was used for all calculations. For each molecule, the geometry was fully optimized to achieve the lowest total energy before energy level calculation, and all possible spin multiplicities were explored (S=0, 1, 2), among which we chose the one with the lowest energy for comparison between different molecules.

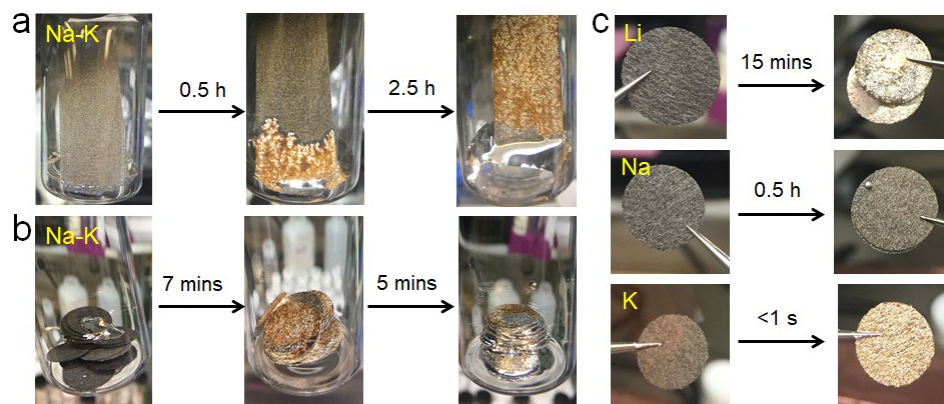


Figure S1. (a) Photos of Na-K liquid alloy diffusing along a carbon paper strip at room temperature after immersion of one end in the liquid alloy. (b) Photos of Na-K liquid alloy diffusing in many stacked carbon paper discs at room temperature after mixing together. (c) Photos of carbon paper discs before and after immersion in molten Li, Na and K metals for a specific time.

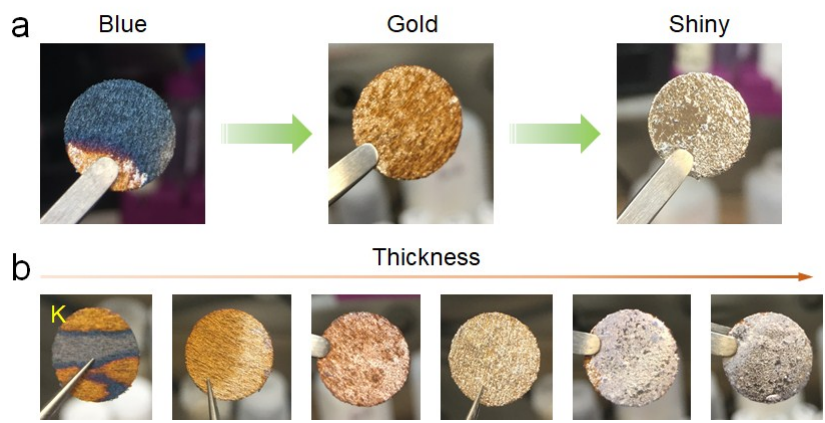


Figure S2. (a) Photos of carbon paper with the color change after immersion in Na-K liquid alloy. (b) Photos of MK-G-C electrode preparation with the increasing amount of molten K absorbed in the carbon paper disc.

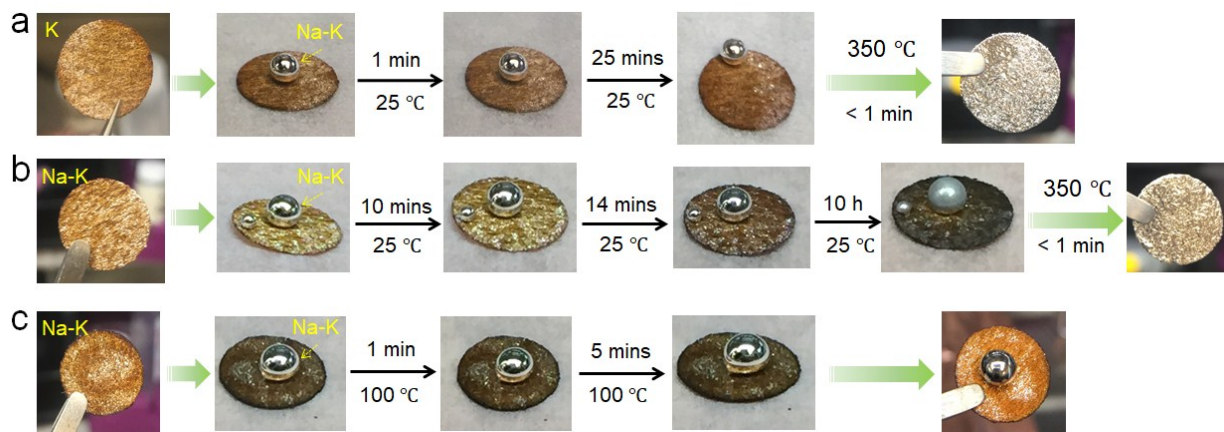


Figure S3. (a) Photos of a Na-K liquid drop on the gold MK-G-C electrode at room temperature. The Na-K liquid is blocked on the surface of the gold MK-G-C electrode. After heating to high temperature (350 °C), the Na-K liquid infuse into the electrode quickly. (b) Photos of a Na-K liquid drop on the gold NaK-G-C electrode at room temperature. The Na-K liquid is also blocked on the surface of the gold NaK-G-C electrode. And after a period of time, the surface of Na-K liquid drop turns to be matte, indicating the formation of oxides. Similarly, after heating at 350 °C, the Na-K liquid infuse into the electrode quickly. (c) Photos of a Na-K liquid drop on the gold NaK-G-C electrode at the intermediate temperature (100 °C). The Na-K is still blocked on the surface of the gold NaK-G-C electrode if the applied temperature is not enough to remove the existed impurities (oxides).

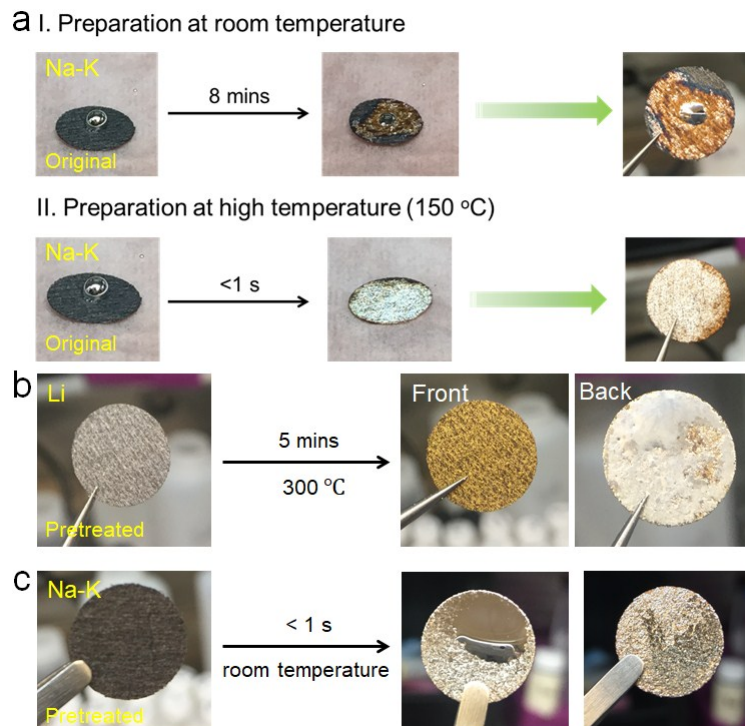


Figure S4. (a) Photos of Na-K liquid alloy diffusing into original carbon paper discs at room temperature or high temperature (150 °C). (b) Photos of molten Li diffusing into a carbon paper disc at high temperature (300 °C). (c) Photos of Na-K liquid alloy diffusing into a carbon paper disc at room temperature (~25 °C). The used carbon paper discs (b and c) are pretreated in ethanol and completely dried at 120 °C.

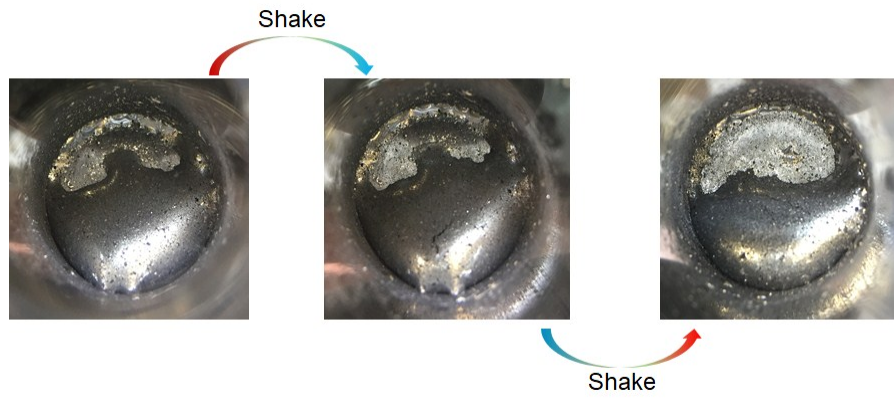


Figure S5. Photos of state of the oxide layer covering on the surface in the shaking experiment, showing the self-healing behavior of Na-K liquid alloy.

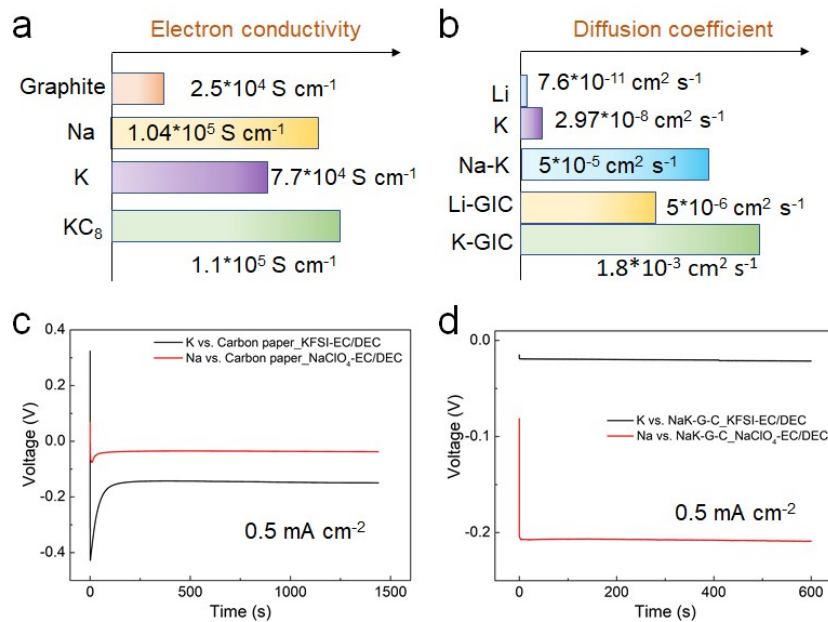


Figure S6. (a) Electron conductivities of graphite, Na liquid, K liquid and graphite intercalation compound KC_8 .^{4,5} (b) Self-diffusion coefficient of Li, K metals and Na-K alloy (373K) and diffusion coefficient of Li and K in the graphitic structure at room temperature.⁶⁻¹¹ (c and d) Galvanostatic Na and K electrodeposition voltage profiles for asymmetric cells (K|Carbon paper, Na|Carbon paper, K|NaK-G-C and Na|NaK-G-C) measured at a fixed current density of $0.5\ mA\ cm^{-2}$.

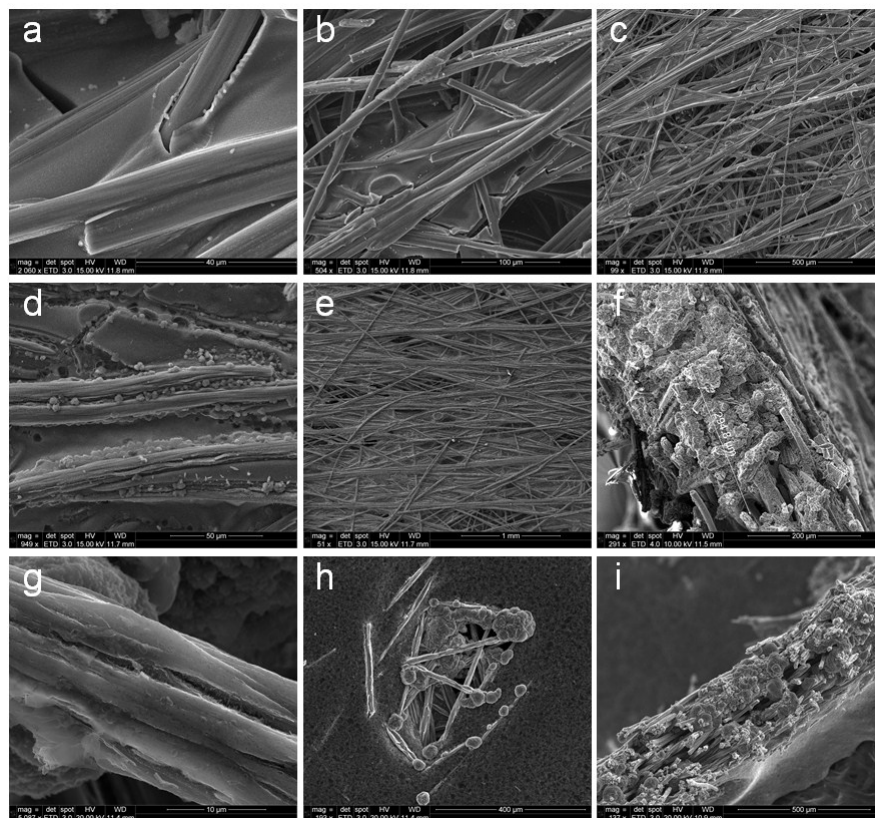


Figure S7. (a,b,c) SEM images of NaK-G-C electrodes with the blue color. (d,e,f) SEM images (d and e) and cross-sectional image (f) of NaK-G-C electrodes with the gold color. (g,h,i) SEM images (g and h) and cross-sectional image (i) of NaK-G-C electrodes with the shiny color.

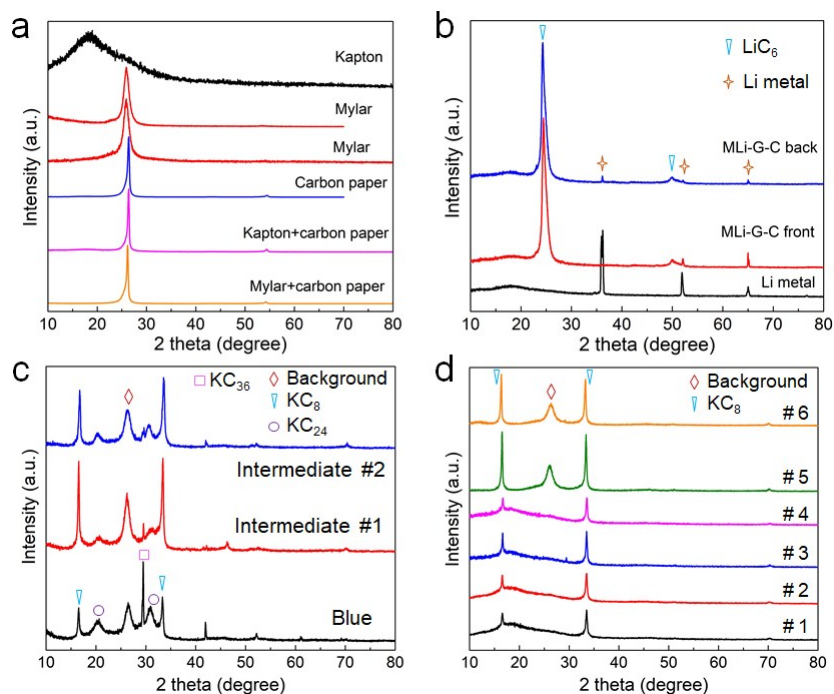


Figure S8. (a) XRD patterns of Kapton and Mylar protective films, and carbon paper discs with or without protective films. (b) XRD patterns of molten Li-GIC-Carbon (MLi-G-C) samples obtained by immersing carbon paper discs into molten Li. (c) XRD patterns of NaK-G-C samples with the blue color and some intermediates. The intermediate samples are prepared by dripping limited Na-K liquids onto carbon paper discs and then quickly transferred to the XRD holder for structure characterizations. (d) XRD patterns of multiple NaK-G-C samples with the gold & shiny colors.

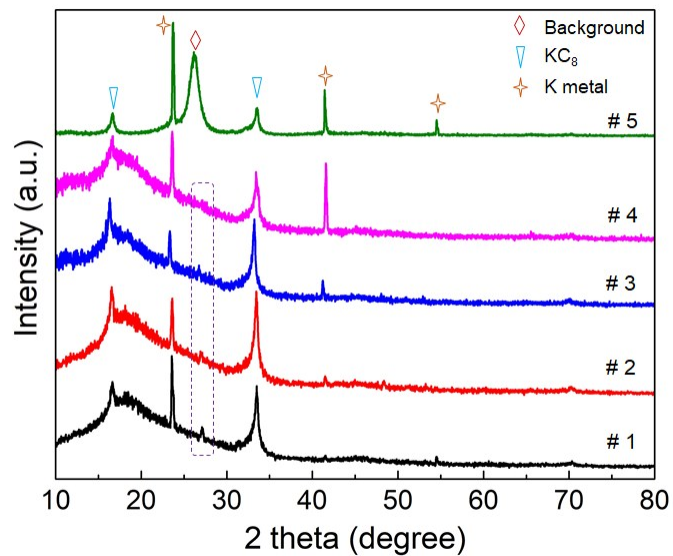


Figure S9. XRD patterns of multiple MK-G-C samples with Kapton or Mylar protective films. The background peak is related to Mylar protective films. The peak inside the gridlines may be attributed to some random stage structure.

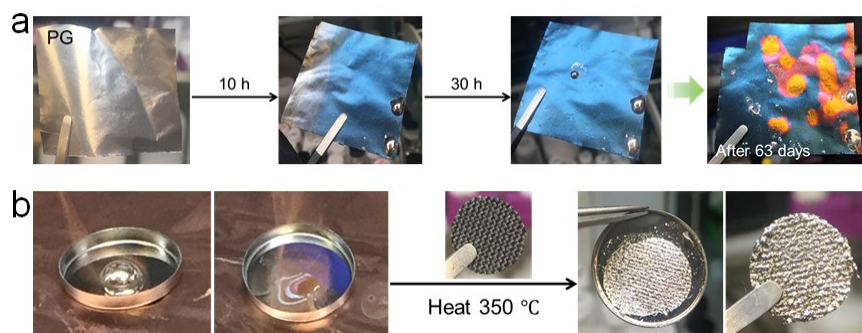


Figure S10. (a) Photos of Na-K liquid alloy diffusing into a PG film at room temperature after Na-K liquid dripped on the surface. **(b)** Photos of Na-K liquid alloy diffusing into a CFC disc at high temperature after immersion in heated Na-K liquid.

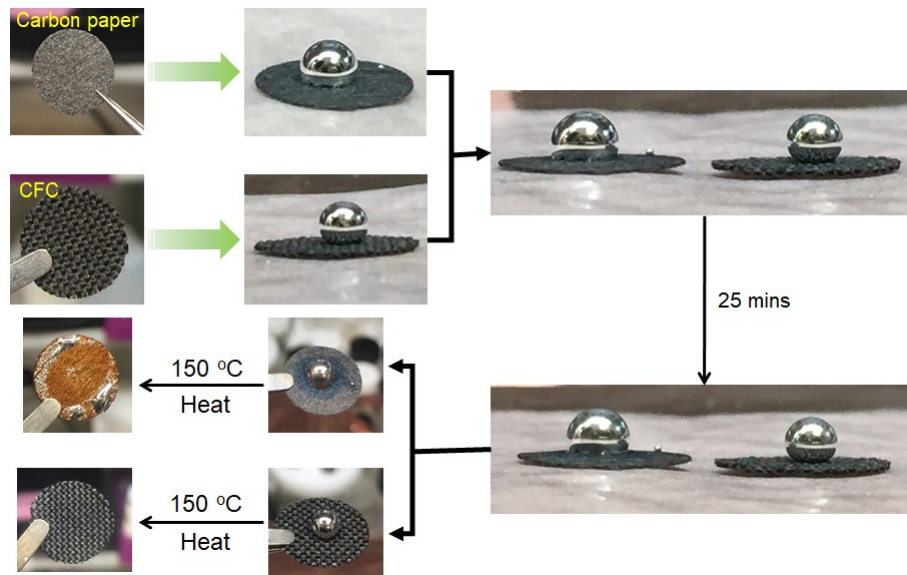


Figure S11. Photos of a Na-K liquid drop on the carbon paper and CFC disc at room temperature. The Na-K liquid has a better wetting behavior on the surface of carbon paper than CFC. The Na-K liquid can gradually infuse into the original carbon paper and the infusion is completed after heating to 150 °C. But for CFC, the Na-K liquid can hardly diffuse into the carbon matrix even after heating to 150 °C. So the much higher temperature will be needed to infuse the Na-K liquid into CFC.

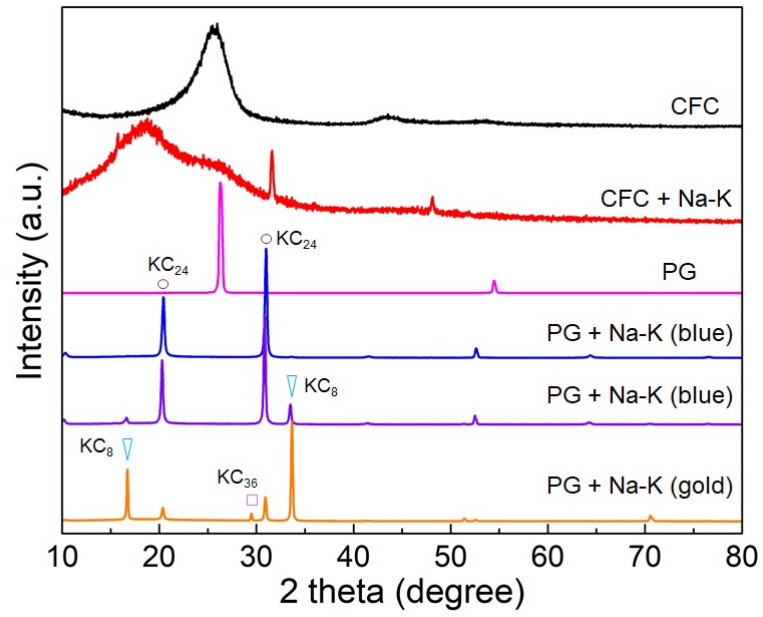


Figure S12. X-ray diffraction patterns of CFC discs and PG films before and after the infusion of Na-K liquid alloy.

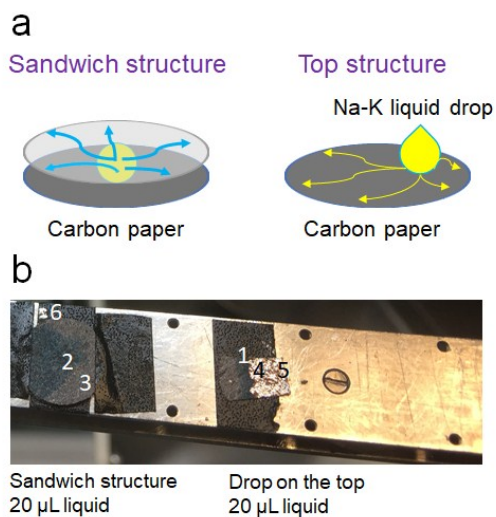


Figure S13. (a) Two special electrodes are designed for the XPS measurement. The sandwich electrode is prepared by dropping 10-20 μL Na-K liquid between two carbon paper pieces and the top electrode is prepared by 10-20 μL on the top surface of a carbon paper disc. **(b)** Photos of obtained electrodes for the XPS analysis (left, sandwich structure; right, top structure). Six specific positions are selected for the XPS measurement (P1, NaK_blue_top; P2, NaK_blue_sandwich; P3, NaK_gold_sandwich; P4, NaK_shiny_top; P5, NaK_grey_top; P6, NaK_liquid drop). Actually, the photo is taken in the beginning in which the diffusion is not completed. In the transfer process, the color becomes gold in the P3 position.

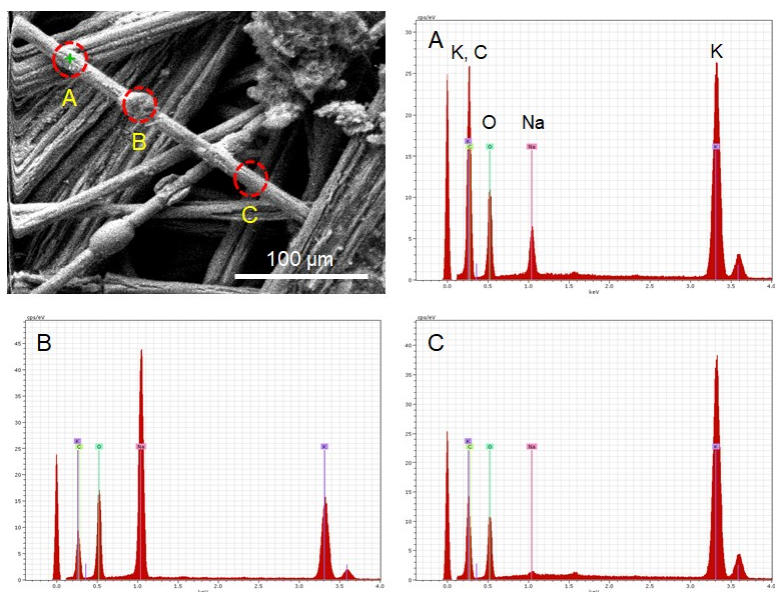


Figure S14. EDS analysis of diffusion of Na-K liquid on the single carbon fiber during the preparation of NaK-G-C electrodes. Three different surface sites selected in the golden NaK-G-C sample are measured. In the C site, only the K signal is detected, confirming the fast diffusion of K in the initial stage. Then, the Na-K alloy is induced to infuse into the carbon matrix and cover on the carbon fibers, which is confirmed by the Na signal detected in both A and B sites. And the Na-K liquid is clearly seen in the B site.

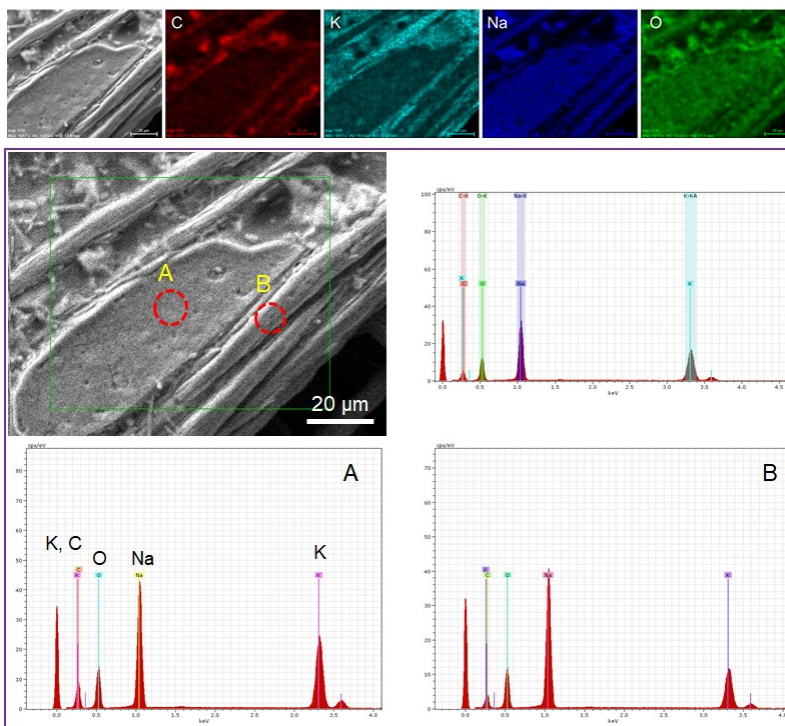


Figure S15. EDS elemental mapping of C, K, Na and O of a selected region in the shiny NaK-G-C electrode. And EDS analysis of distribution of Na and K elements in two different surface sites. A is on the liquid filled in the gap between carbon fibers. B is on the carbon fiber with the formation of GIC. The strong Na signal is detected in all the selected sites, indicating the uniform distribution of Na-K alloy inside the final product.

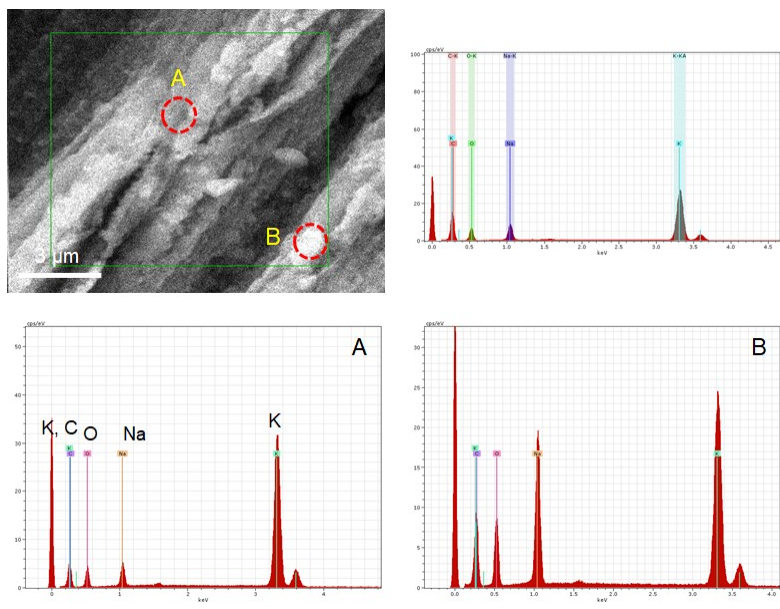


Figure S16. EDS analysis of distribution of Na and K elements on the single carbon fiber in the shiny NaK-G-C sample. Two different surface sites are measured. As shown above, the Na-K alloy coating on the surface of carbon fibers is further confirmed, as indicated by the detected Na signal.

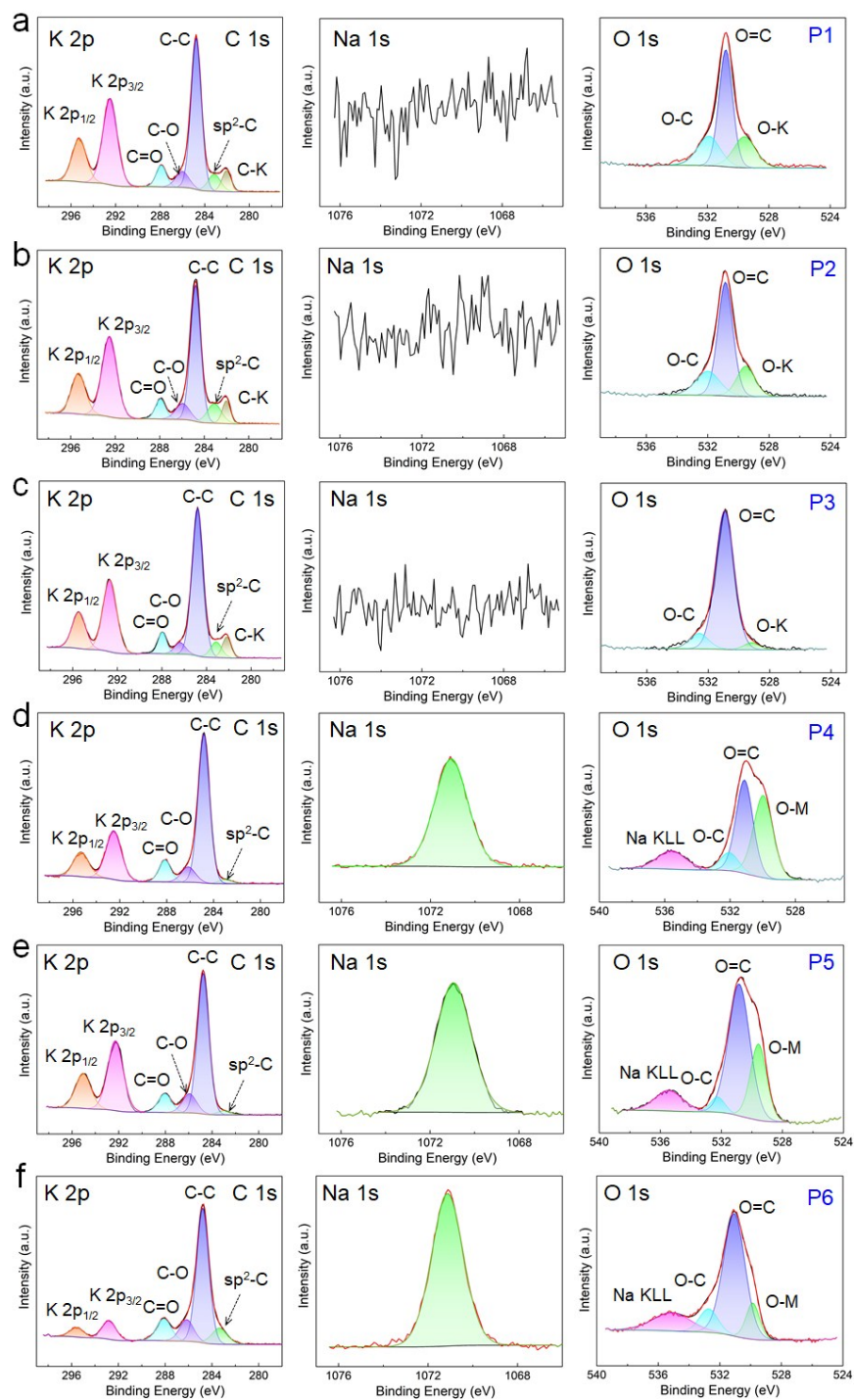


Figure S17. XPS analysis of two designed special electrodes (Figure S14) in six selected positions, C 1s, K 2p, Na 1s, O 1s spectra are presented, including peak deconvolution and assignments. For P1 (blue_top), P2 (blue_sandwich) and P3 (gold_sandwich), the XPS spectra are very similar, implying the diffusion of Na-K liquid inside the carbon matrix is homogeneous. For P4 (shiny_top), P5 (grey_top) and P6 (liquid drop), the XPS spectra are also very similar, which means the liquid covering on the surface of electrode acts the same as the original Na-K liquid.

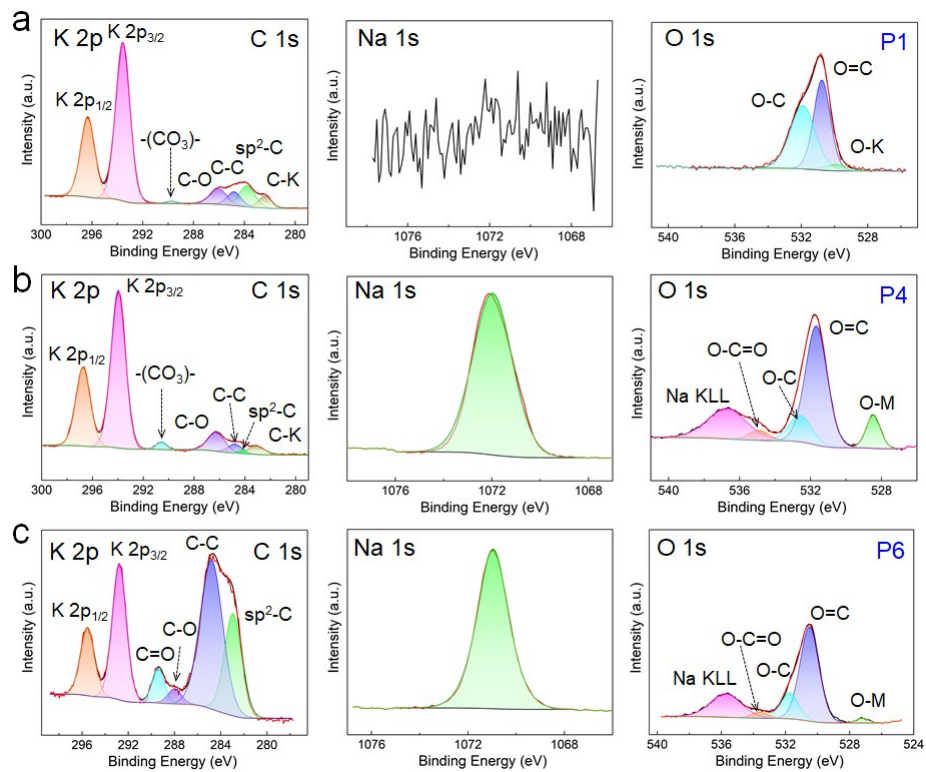


Figure S18. XPS analysis of three selected positions (P1, P4 and P6) after Ar sputtering, C 1s, K 2p, Na 1s, O 1s spectra are presented, including peak deconvolution and assignments.

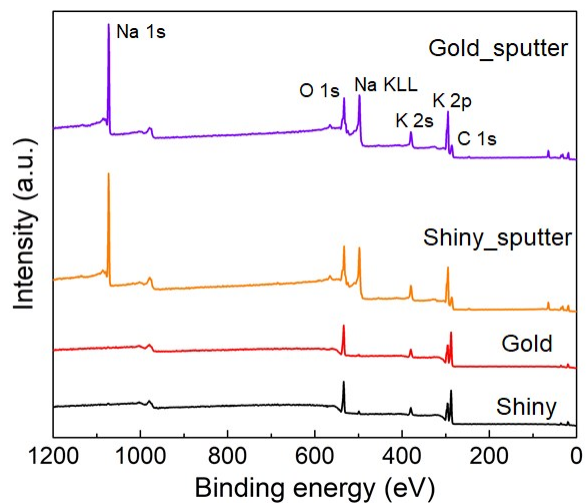


Figure S19. XPS study of the original NaK-G-C electrode. In some cases, the surface is not fully covered by Na-K liquid alloy so two different sites (gold and shiny) are selected for XPS measurement.

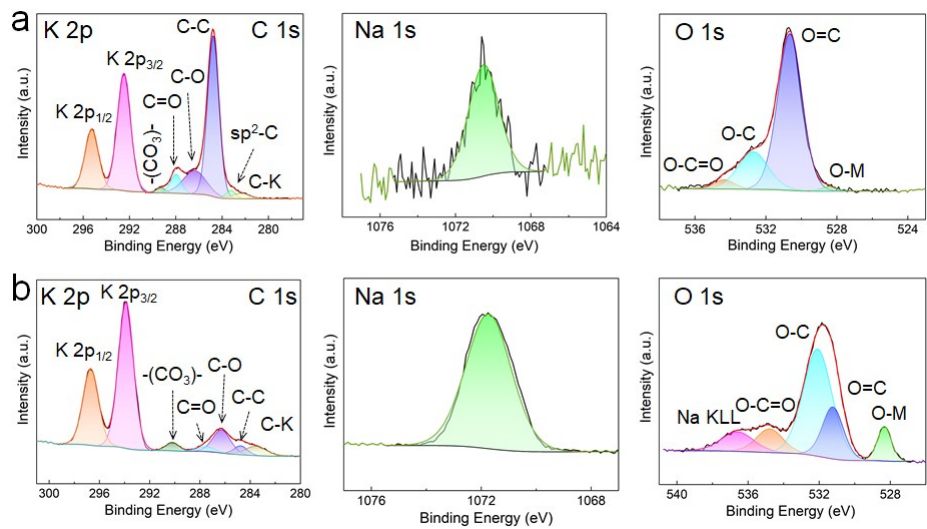


Figure S20. XPS analysis of the shiny site in the NaK-G-C electrode before (up) and after Ar sputtering (down), C 1s, K 2p, Na 1s, O 1s spectra are presented, including peak deconvolution and assignments.

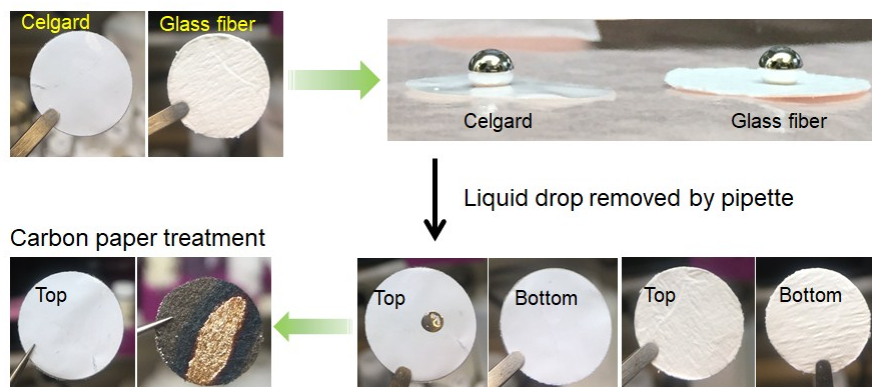


Figure S21. Photos of a Na-K liquid drop on Celgard and glass fiber membranes without absorbing any liquid electrolytes at room temperature. The contact between Na-K liquid and Celgard seems to be better than glass fiber membrane because a small amount of liquid is left on the surface of Celgard after removing by a pipette. And the carbon paper can easily absorb the Na-K liquid when contacting with Celgard, indicating that the direct short circuit by the penetration of Na-K should be difficult.

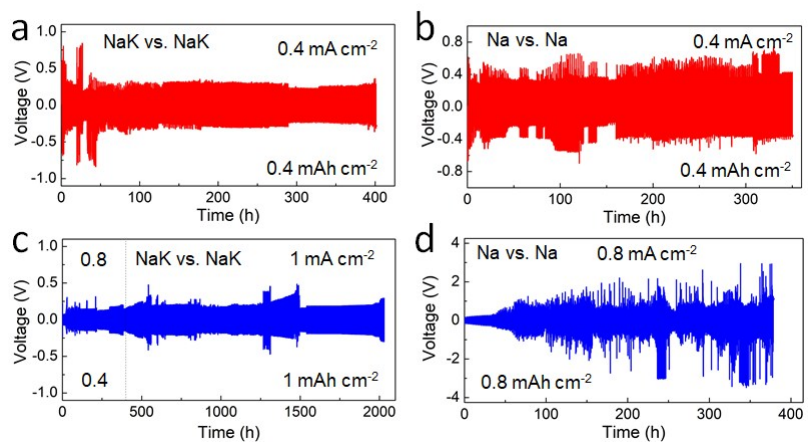


Figure S22. Galvanostatic stripping/deposition voltage profiles in the same Na-ion electrolyte (NaClO_4 EC/DEC) for the NaK-G-C|NaK-G-C and pristine Na|Na symmetric cells at different current densities.

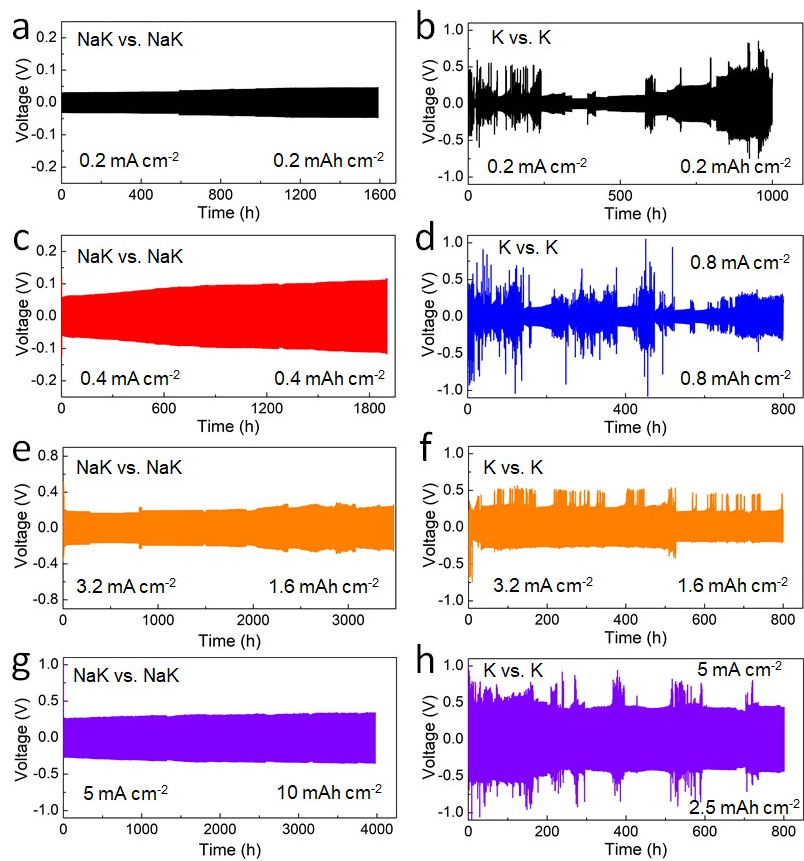


Figure S23. Galvanostatic stripping/deposition voltage profiles in the same K-ion electrolyte (KFSI EC/DEC) for the NaK-G-C|NaK-G-C and pristine K|K symmetric cells at different current densities.

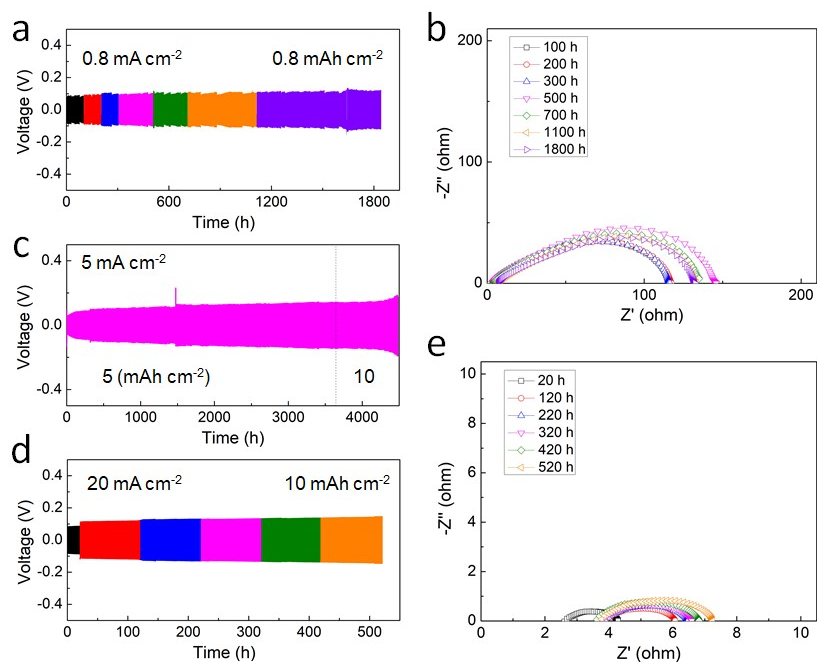


Figure S24. Galvanostatic stripping/deposition voltage profiles in the K-ion electrolyte (KFSI EC/DEC) for the NaK-G-C|NaK-G-C symmetric cells at different current densities. And the corresponding Nyquist plots (**b** and **e**) of the symmetric cells (**a** and **d**), respectively, during the stripping/deposition.

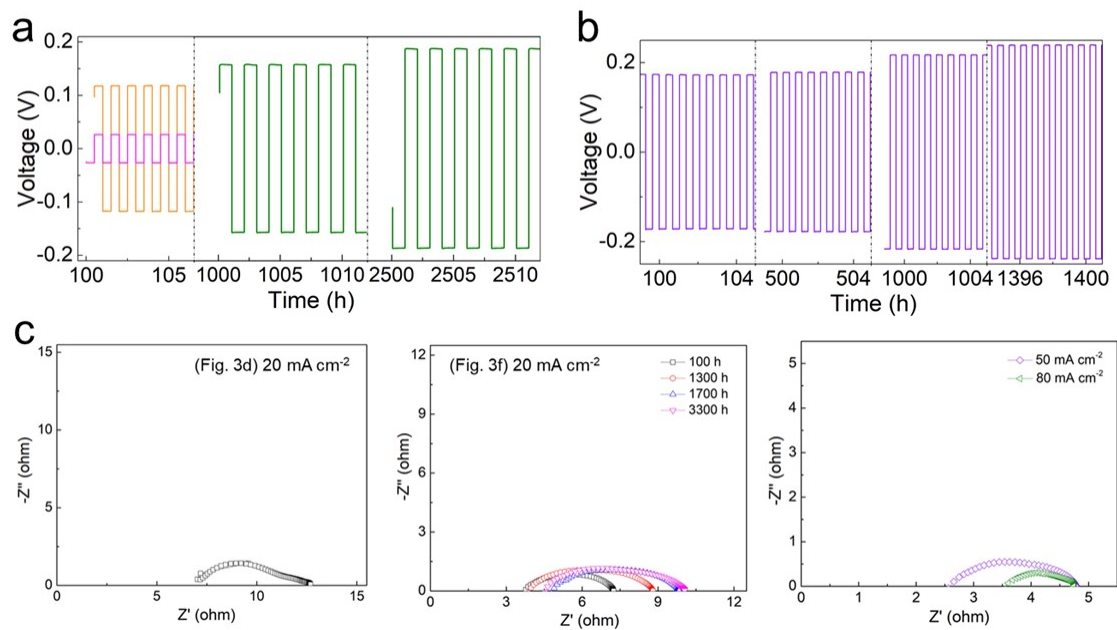


Figure S25. The enlarged overpotentials of symmetric cells cycled at 20 (a) and 50 mA cm⁻² (b) in the selected regions corresponding to main Fig. 3f-g. (c) The corresponding Nyquist plots of the symmetric cells cycled at high current densities (Fig. 3d, f, g and h).

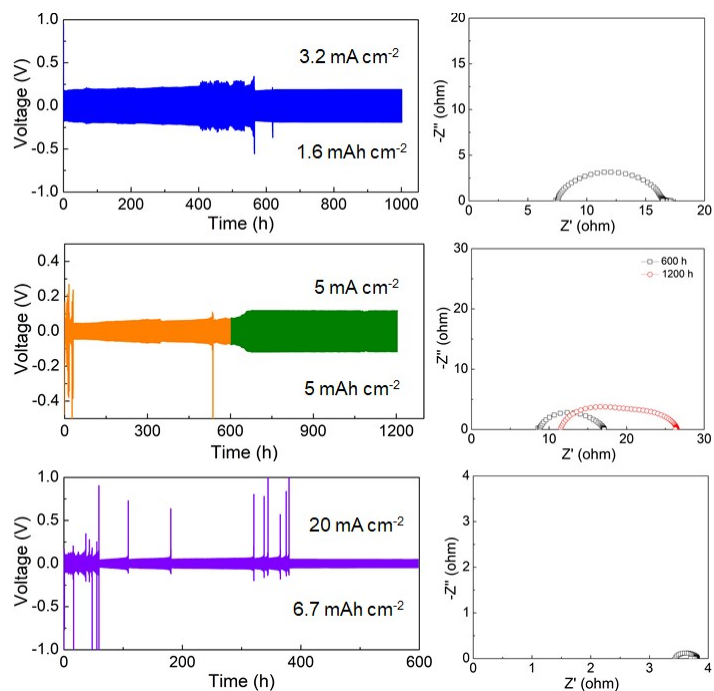


Figure S26. Galvanostatic stripping/deposition voltage profiles in the K-ion electrolyte (KFSI EC/DEC) for the MK-G-C|MK-G-C symmetric cells at different current densities. And the corresponding Nyquist plots of the symmetric cells after cycling or at specific cycles.

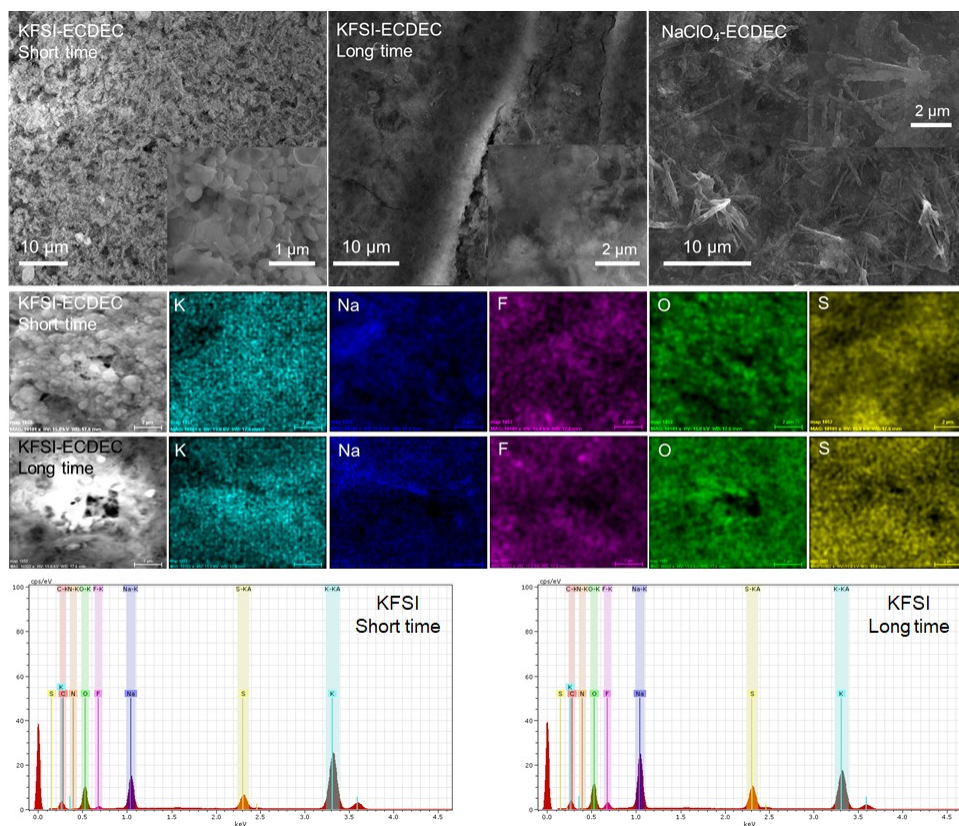


Figure S27. SEM images of cycled NaK-G-C electrodes obtained in KFSI EC/DEC (short time and long time) and NaClO₄ EC/DEC electrolytes. The Insets show the high magnification SEM images. The EDS elemental mapping and analysis of K, Na, F, O and S of selected regions in the cycled NaK-G-C electrodes using KFSI EC/DEC electrolytes are also presented.

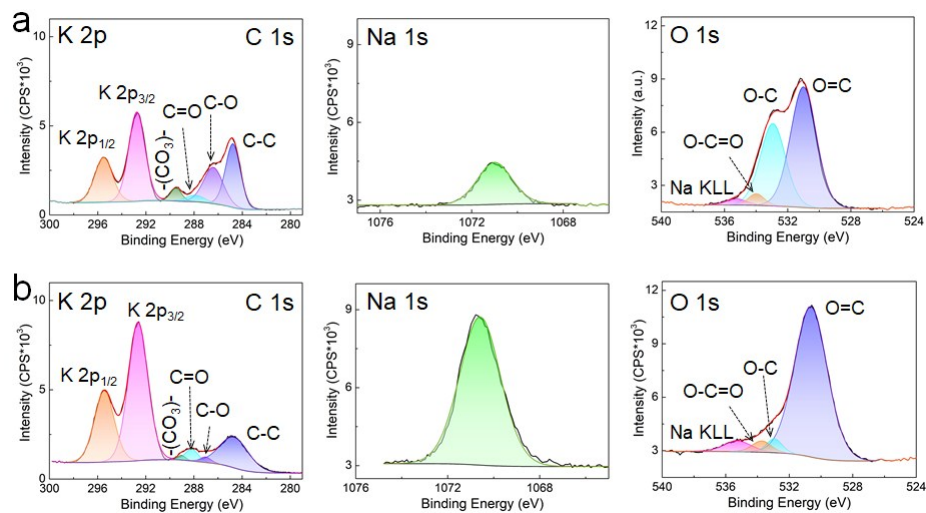


Figure S28. XPS analysis of the cycled NaK-G-C electrode obtained from NaClO₄ EC/DEC electrolytes before (up) and after Ar sputtering (down), C 1s, K 2p, Na 1s, O 1s spectra are presented, including peak deconvolution and assignments.

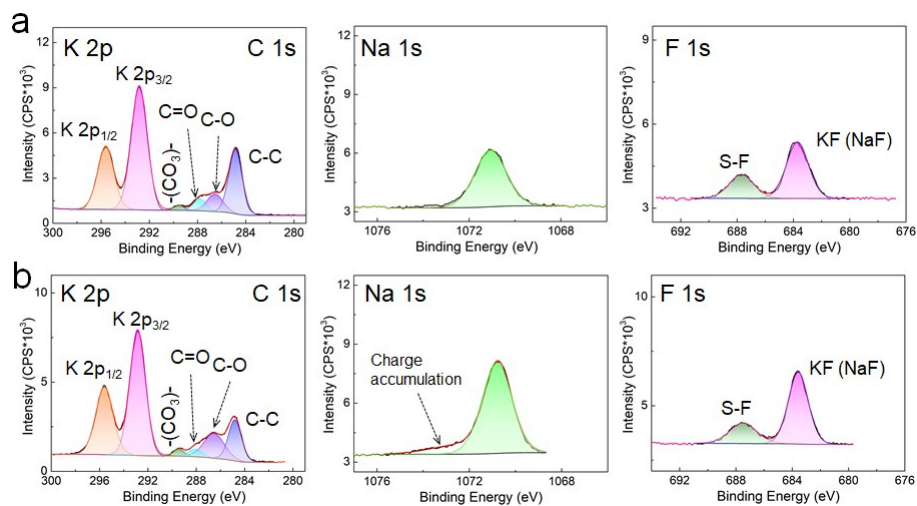


Figure S29. XPS analysis of the cycled NaK-G-C electrode obtained from KFSI EC/DEC electrolytes after a short time (up) and long time (down) without the Ar sputtering, C 1s, K 2p, Na 1s, F 1s spectra are presented, including peak deconvolution and assignments.

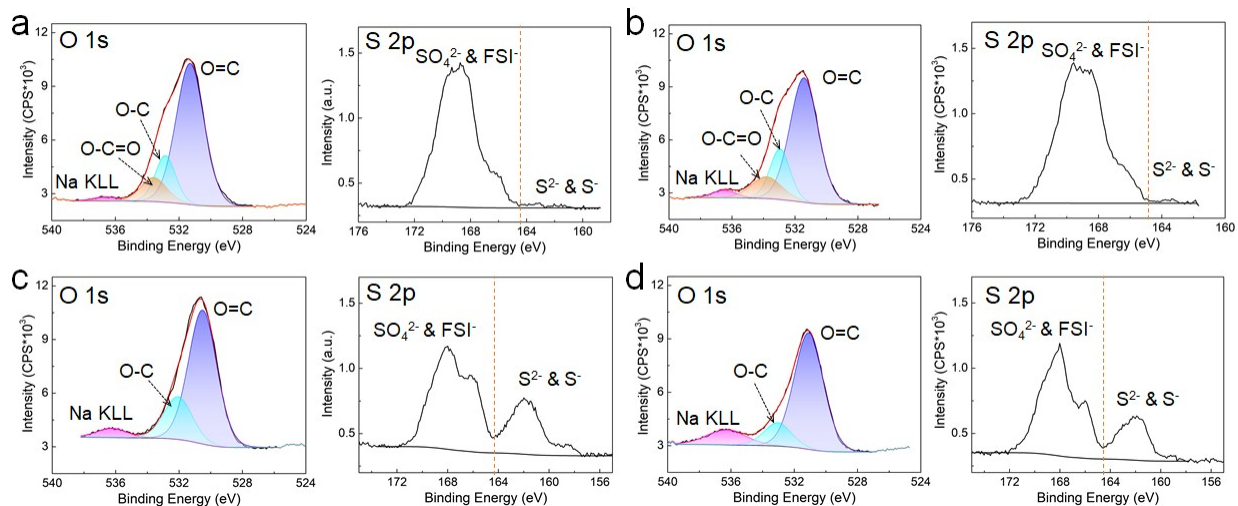


Figure S30. (a and b) XPS characterization of O 1s and S 2p peaks for the NaK-G-C electrodes cycled in the KFSI EC/DEC electrolyte after a short time (a) and long time (b) without the Ar sputtering. (c and d) XPS characterization of O 1s and S 2p peaks for the NaK-G-C electrodes cycled in the KFSI EC/DEC electrolyte after a short time (c) and long time (d) with the Ar sputtering.

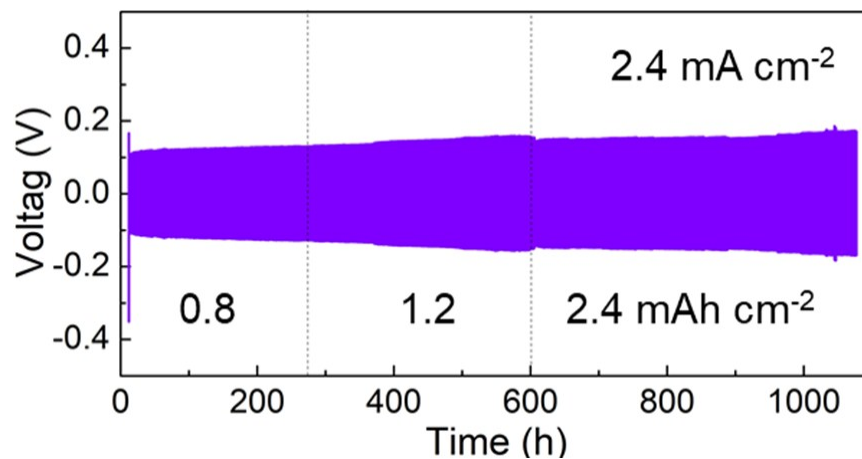


Figure S31. Galvanostatic stripping/deposition voltage profiles in the K-ion electrolyte (KFSI EC/DEC) for the NaK-G-C|NaK-G-C symmetric cells at the current density of 2.4 mA cm^{-2} . After cycling, the NaK-G-C electrode is used for the XPS analysis (long time).

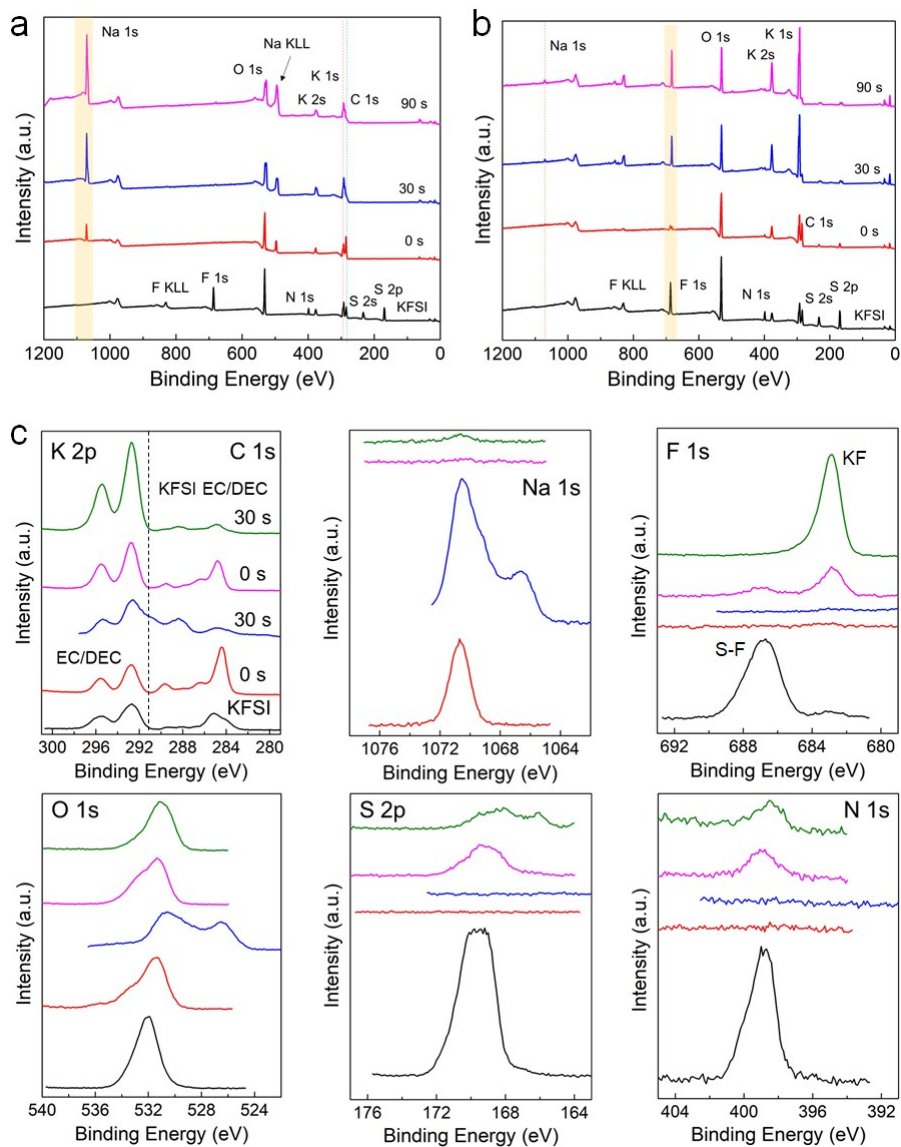


Figure S32. XPS study of NaK-G-C electrodes after immersed in EC/DEC solvents (a) or KFSI EC/DEC electrolytes (b) before and after Ar sputtering. The XPS analysis of KFSI salts is also presented as the reference. (c) The corresponding high-resolution K 2p, C 1s, Na 1s, F 1s, O 1s, S 2p and N 1s spectra before and after 30s Ar sputtering are presented.

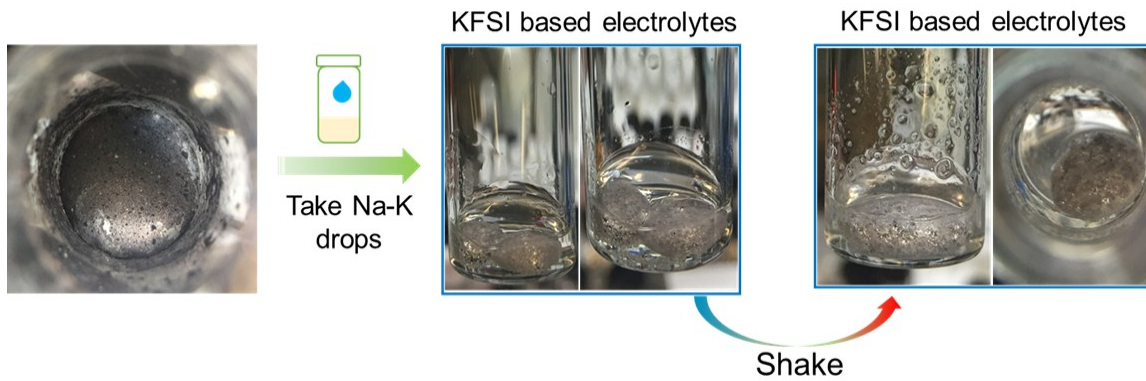


Figure S33. The shaking experiment of Na-K liquid alloy in the KFSI EC/DEC electrolytes, showing the self-healing behavior with the formation of SEI layer.

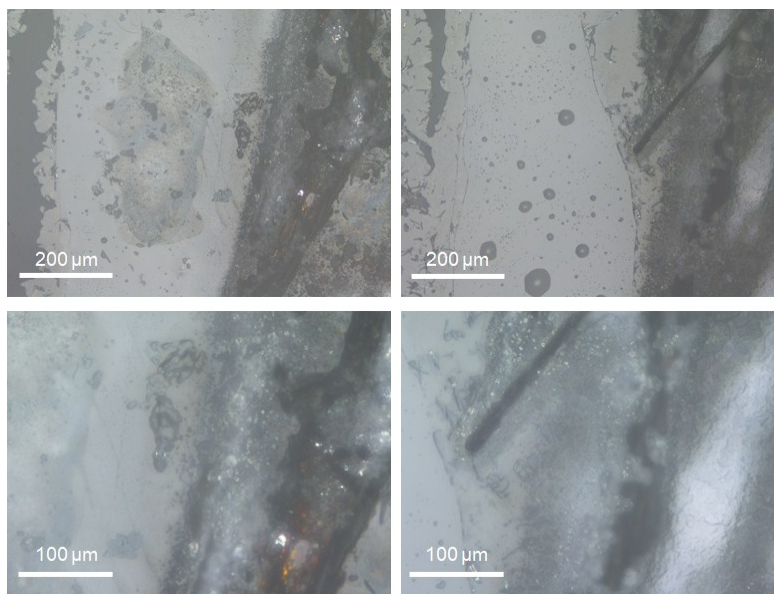


Figure S34. Optical microscopy images of interface of MK-G-C electrodes cycled in the transparent cell for 20 cycles at the current density of 5 mA cm⁻².

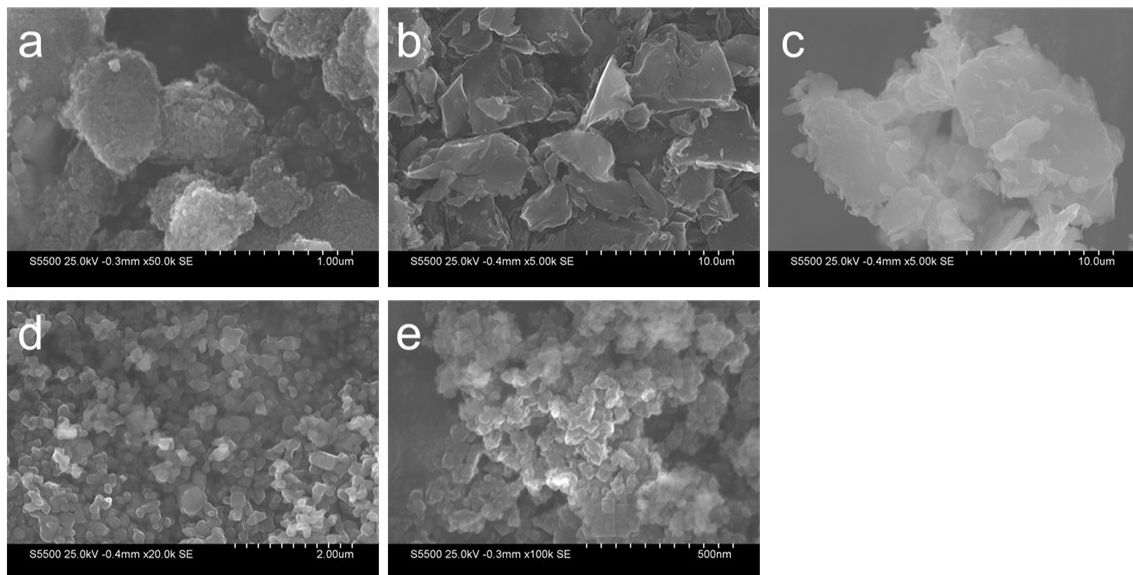


Figure S35. SEM images of T-Nb₂O₅/rGO (a), AC (b), bulk VOPO₄ (c), Na₂MnFe(CN)₆ (d) and K₂MnFe(CN)₆ (e) cathode materials.

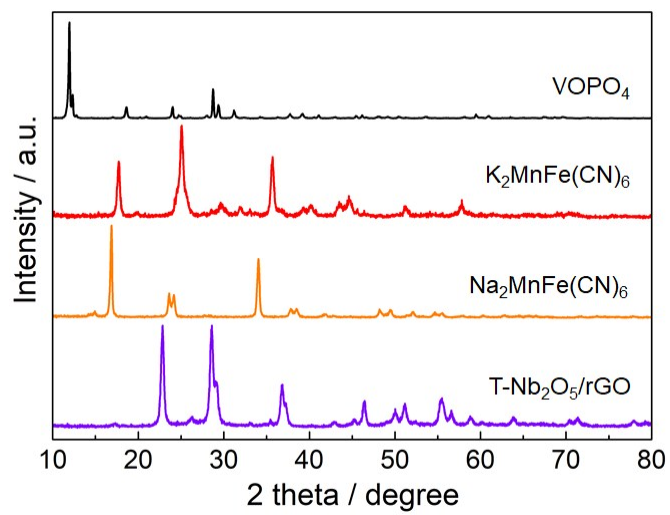


Figure S36. XRD patterns of different cathode materials.

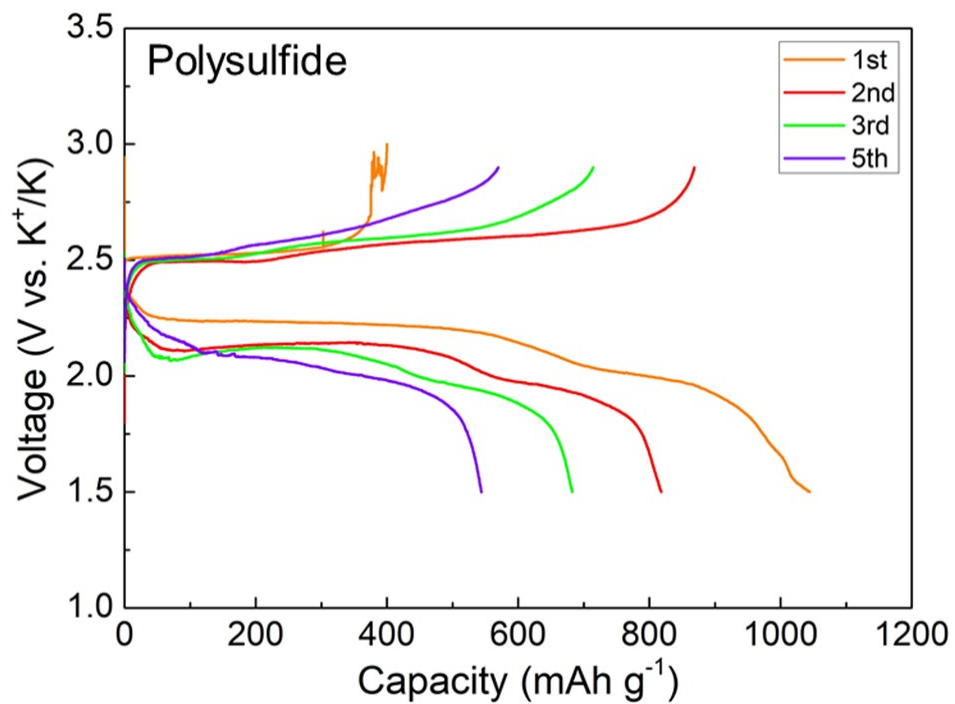


Figure S37. The Galvanostatic charging and discharging profiles of room-temperature K-S battery using NaK-G-C anode and polysulfide cathode at 0.05 C (1C = 1600 mA g⁻¹).

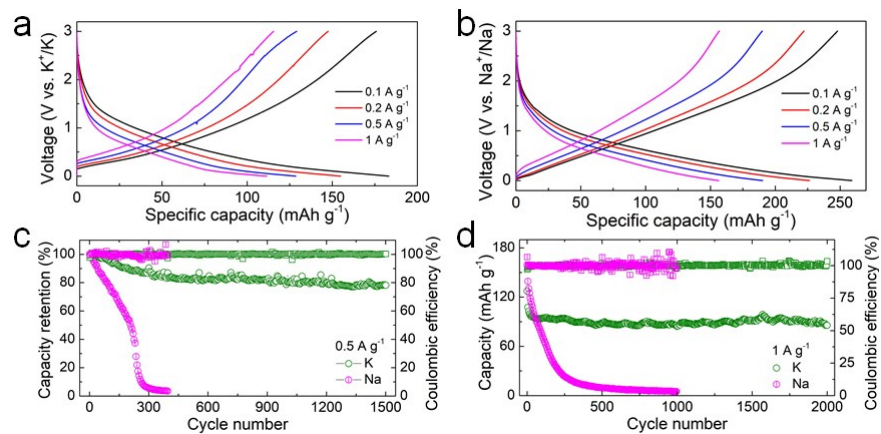


Figure S38. (a and b) Charge/discharge curves of the full cell using T-Nb₂O₅/rGO as the cathode and NaK-G-C as the anode in K-ion (a, KFSI EC/DEC) and Na-ion (b, NaClO₄ PC with 2 wt% FEC) electrolytes. (c and d) Cycling performance with discharge capacity and coulombic efficiency of full cells in K-ion and Na-ion electrolytes at different current densities.

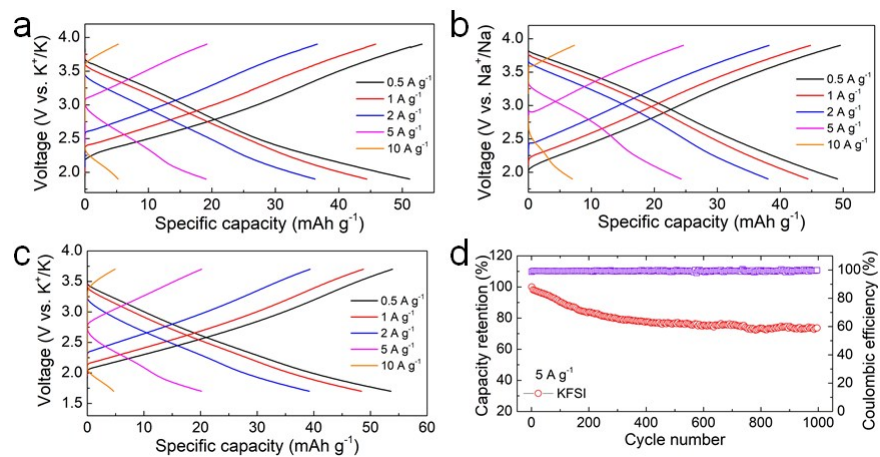


Figure S39. (a,b,c) Charge/discharge curves of the NaK-G-C|AC hybrid capacitors in K-ion (KFSI EC/DEC) (a and c) and Na-ion (NaClO₄ PC with 2 wt% FEC) (b) electrolytes at different current densities. The operating voltage window of (a) and (c) is different. (d) Cycling performance of the NaK-G-C|AC hybrid capacitor in the K-ion (KFSI EC/DEC) electrolyte at the current density of 5 A g⁻¹.

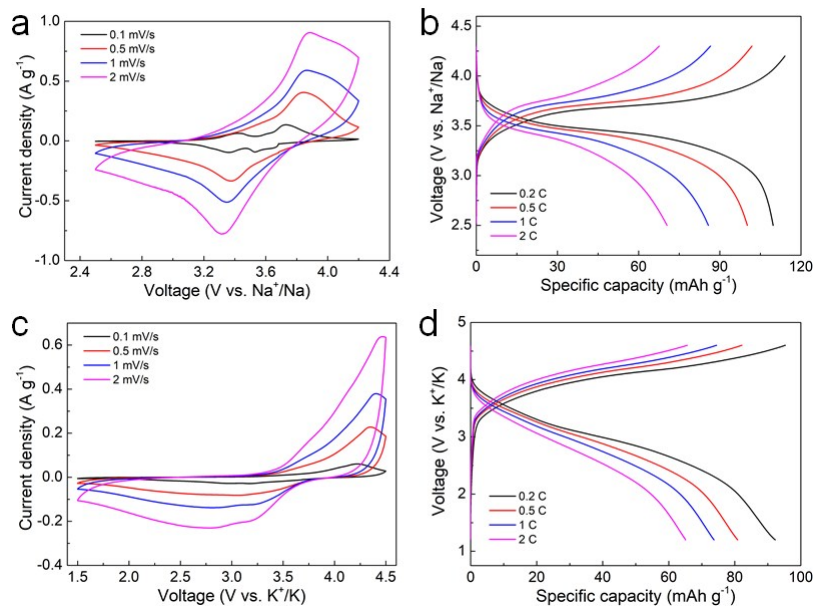


Figure S40. (a) CV curves of NaK-G-C|VOPO₄ cells in Na-ion (NaClO₄ PC with 2 wt% FEC) electrolytes at various scan rates, from 0.1 to 2 mV/s. (b) Charging and discharging curves of NaK-G-C|VOPO₄ cells in Na-ion (NaClO₄ PC with 2 wt% FEC) electrolytes at various C rates. (c) CV curves of NaK-G-C|VOPO₄ cells in K-ion (KClO₄ PC with 2 wt% FEC) electrolytes at various scan rates, from 0.1 to 2 mV/s. (d) Charging and discharging curves of NaK-G-C|VOPO₄ cells in K-ion (KClO₄ PC with 2 wt% FEC) electrolytes at various C rates.

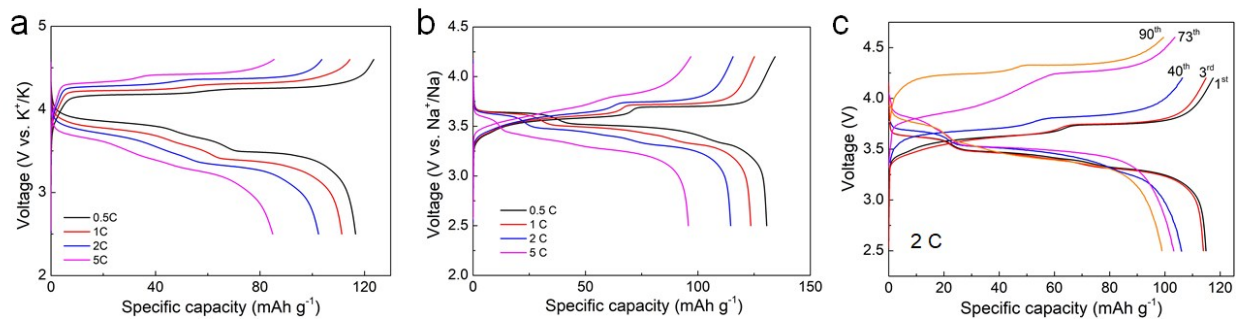


Figure S41. (a and b) Charge/discharge curves of the NaK-G-C|K₂MnFe(CN)₆ (a) and NaK-G-C|Na₂MnFe(CN)₆ (b) cells at different rates. 1C for K₂MnFe(CN)₆ is 160 mA g⁻¹; 1C for Na₂MnFe(CN)₆ is 120 mA g⁻¹. (c) Evolution of voltage profile of NaK-G-C|Na₂MnFe(CN)₆ cell with cycle number at 2 C.

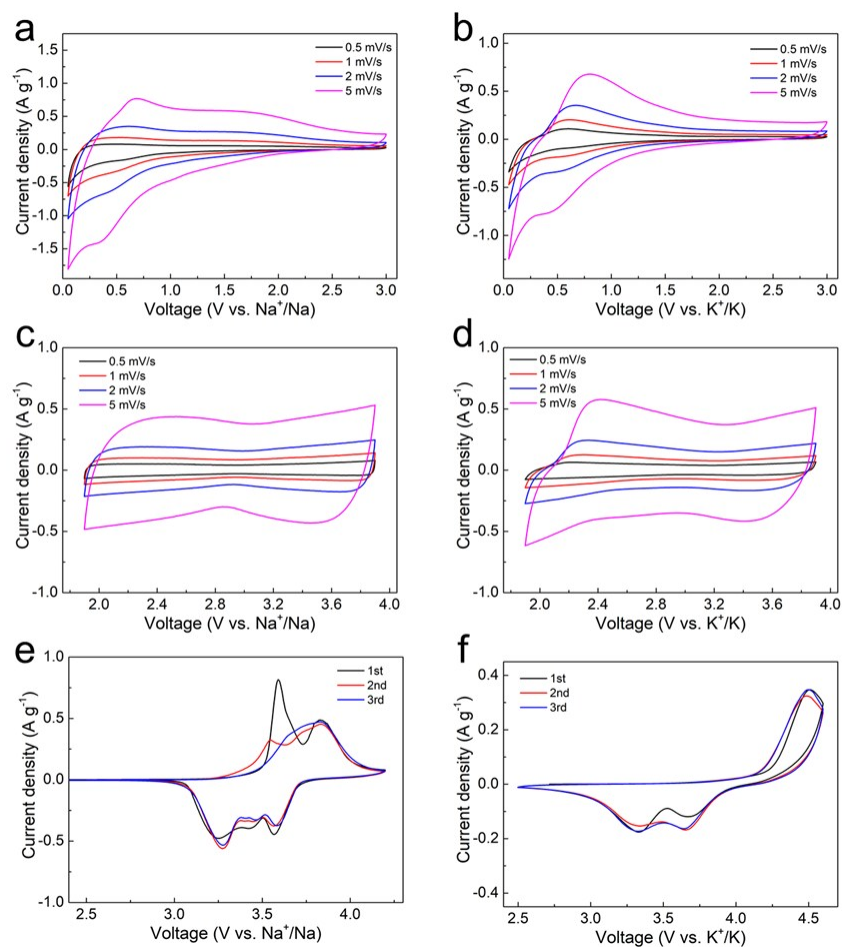


Figure S42. (a and b) CV curves of the full cell using T-Nb₂O₅/rGO as the cathode and NaK-G-C as the anode in Na-ion (a, NaClO₄ PC with 2 wt% FEC) and K-ion (b, KFSI EC/DEC) electrolytes at various scan rates. (c and d) CV curves of NaK-G-C|AC cells in Na-ion (c, NaClO₄ PC with 2 wt% FEC) and K-ion (d, KFSI EC/DEC) electrolytes at various scan rates. (e and f) CV curves of NaK-G-C|Na₂MnFe(CN)₆ or NaK-G-C|K₂MnFe(CN)₆ cells in Na-ion (e, NaClO₄ PC with 2 wt% FEC) or K-ion (f, KClO₄ PC with 2 wt% FEC) electrolytes, respectively, at the scan rate of 0.5 mV s⁻¹.

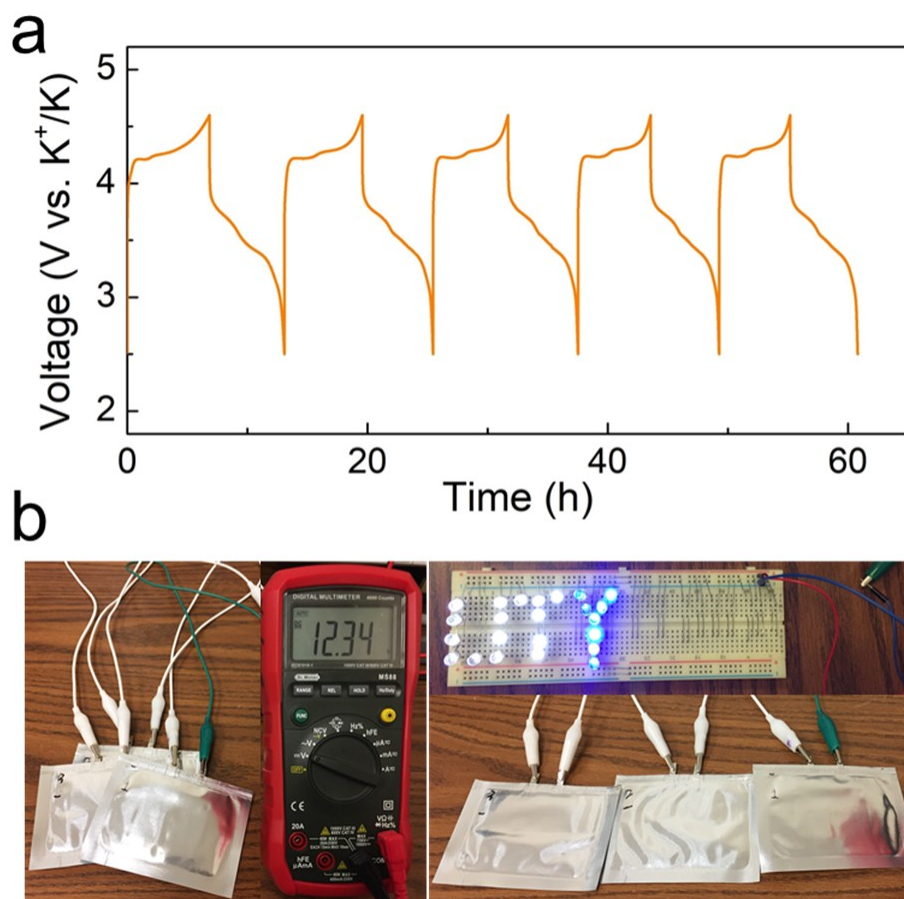


Figure S43. (a) The galvanostatic charging and discharging curves of the pouch-type battery using the large-area NaK-G-C anode and $\text{K}_2\text{MnFe}(\text{CN})_6$ cathode at the C rate of 0.1 C with the operating voltage window of 2.5 V-4.6 V. (b) The pouch battery in series can provide a high voltage of 12.3 V and can also light a series of white and blue LEDs.

References

1. Y. Zhu, L. Peng, D. Chen and G. Yu, *Nano Lett.*, 2016, **16**, 742-747.
2. L. Xue, Y. Li, H. Gao, W. Zhou, X. Lü, W. Kaveevivitchai, A. Manthiram and J. B. Goodenough, *J. Am. Chem. Soc.*, 2017, **139**, 2164-2167.
3. L. Wang, Y. Lu, J. Liu, M. Xu, J. Cheng, D. Zhang and J. B. Goodenough, *Angew. Chem. Int. Ed.*, 2013, **52**, 1964-1967.
4. M. S. Dresselhaus and G. Dresselhaus, *Adv. in Phys.*, 2002, **51**, 1-186.
5. N. Cusack, *Reports on progress in physics*, 1963, **26**, 361.
6. E. Dologlou, *Glass Physics and Chemistry*, 2010, **36**, 570-574.
7. L. Mandelkort and J. T. Yates Jr, *The Journal of Physical Chemistry C*, 2012, **116**, 24962-24967.
8. K. Persson, V. A. Sethuraman, L. J. Hardwick, Y. Hinuma, Y. S. Meng, A. Van Der Ven, V. Srinivasan, R. Kostecki and G. Ceder, *J. Phys. Chem. Lett.*, 2010, **1**, 1176-1180.
9. J. Mundy, T. Miller and R. Porte, *Phys. Rev. B*, 1971, **3**, 2445.
10. J. Renard, M. Lundeberg, J. Folk and Y. Pennec, *Phys. Rev. Lett.*, 2011, **106**, 156101.
11. A. Baumketner and Y. Chushak, *J. Phys.: Condens. Matter*, 1999, **11**, 1397.